Bol. Soc. Paran. Mat.
©SPM – E-ISSN-2175-1188
SPM: www.spm.uem.br/bspm

(3s.) **v. 2025 (43)** : 1–14.
ISSN-0037-8712
doi:10.5269/bspm.76499

Hybrid Quartic B-Spline Method for Solving Time Fractional Differential Equations

Fahad K. Nashmi* and Bushra A. Taha

ABSTRACT: This paper presents a novel hybrid B-spline method (HB-spline) collocation method for the efficient and precise resolution of time-fractional partial differential equations (TFPDEs). Our approach models anomalous diffusion using the Caputo fractional derivative, discretising the temporal fractional term with a high-order finite difference approximation and employing quartic B-spline basis functions in the spatial domain, enhanced by a variable shape parameter, θ. A comprehensive Fourier stability analysis for fractional orders $\omega \in (1, 2]$ establishes that the proposed HB-spline method is unconditionally stable. We evaluate its performance by applying the method to both linear and nonlinear TFPDEs and comparing the numerical results with established exact solutions. The HB-spline method demonstrates enhanced convergence rates and lower computational expenses, as evaluated by L^2 and L^∞ error norms. The incorporation of the hybrid shape parameter θ facilitates adaptive regulation of the spline's curvature, providing increased flexibility and accuracy in representing intricate solution profiles.

Key Words: Caputo time-fractional derivative, finite difference method, quartic B-spline method, quartic trigonometric B-spline, hybrid B-spline method, diffusion wave equations, reaction and damping.

Contents

1. Introduction

Fractional calculus (FC) broadens the traditional concepts of differentiation and integration to encompass non-integer orders. In fact, FC is an extension of classical calculus [10,31,30,32,35]. Sometimes, fractional models behave more harmoniously than classical models. Therefore, many methods have been developed to deal with these models, and researchers have continued to develop these techniques constantly to obtain high accuracy [42]. Recently, the application of fractional operators to model intricate processes in physics, engineering, biology, and other fields has attracted considerable interest and yielded impressive outcomes [4,8,15,26,25,33,29]. Fractional calculus serves as an essential instrument in science and engineering, facilitating the development of fractional differential equations (FDEs) that inherently include memory and hereditary effects. In the last three to four decades, extensive research on FC and FDEs has demonstrated their enhanced ability compared to integer order models to accurately represent phenomena ranging from local to nonlocal behaviour and transitions between wave-like propagation and diffusive dynamics. Moreover, the fractional order functions as a variable parameter, providing enhanced adaptability for optimisation and performance refinement in multiphysics simulations. Unsurprisingly, these fractional-order methodologies have been extensively utilised in various applications, including image processing, denoising, encryption, and more [3,9,24,22,27,28].

It is widely recognised that the majority of time-fractional differential equations (TFDEs), particularly those containing nonlinear or inhomogeneous components, lack closed-form solutions. In recent years, the

* Corresponding author.
2010 *Mathematics Subject Classification:* 35R11, 65M70, 65D07, 26A33, and 34A08.
Submitted April 23, 2025. Published October 29, 2025

importance of time-fractional partial differential equations (TFPDEs) has increased significantly due to their application in various domains, including signal processing, electromagnetic control theory, electrical network analysis, multidimensional fluid dynamics, and mathematical biology [43,40,36]. Generally, acquiring precise analytic solutions for TFDEs through traditional methods continues to be a significant challenge. As a result, numerous researchers have invested significant effort in developing numerical schemes that are both practically applicable and capable of providing high-accuracy approximations [1,7,37,14,13]. To examine TFDEs, we utilise the subsequent prototype model:

$$\begin{aligned} &\frac{\partial^{\omega} v(r,s)}{\partial s^{\omega}} + \eta \frac{\partial v(r,s)}{\partial s} + \lambda v(r,s) - \frac{\partial^2 v(r,s)}{\partial r^2} = G(v(r,s)) + \phi(r,s), \\ &(r,s) \in \Omega \times (0,S], \ v(r,0) = \zeta_0(r), \quad \frac{\partial v(r,0)}{\partial s} = \zeta_1(r), \qquad r \in \Omega, \\ &v(c,s) = \varsigma_0(s) \quad \textit{and} \quad v(d,s) = \varsigma_1(s). \end{aligned} \tag{1.1}$$

where, $G(v(r,s)) : \mathbb{R} \longrightarrow \mathbb{R}$, is nonlinear with regard to $v(r,s)$, $r \in [c,d]$ and $s \in [0,S]$. while, $\phi(r,s) : [c,d] \times [0,S] \longrightarrow \mathbb{R}$, $\varsigma_0(s), \varsigma_1(s) : [0,S] \longrightarrow \mathbb{R}$ $\zeta_0(r), \zeta_1(r) : [c,d] \longrightarrow \mathbb{R}$. Actually, each of the aforementioned functions needs to be provided. It is important to note that η represents the response term parameter and λ represents the damping term parameter. It is necessary to define the fractional derivative

$$\frac{\partial^{\omega} v(r,s)}{\partial s^{\omega}} = \frac{1}{\Gamma(n-\omega)} \int_c^s \frac{\partial^n v(r,\epsilon)}{\partial \epsilon^n} (s-\epsilon)^{\omega-n+1} \tag{1.2}$$

where, $\Gamma(n-\omega)$ is the Gamma function, which has the following definition

$$\Gamma(n-\omega) = \int_0^{\infty} r^{n-\omega-1} e^{-r} dr, \quad (\mathbb{R}(\omega) > 0). \tag{1.3}$$

Fractional diffusion wave equation have received great attention in physics, such as electromagnetism. These equations fall under the area of fractional order partial differential models [2]. By substituting a real number ω for the exponent of the second derivative of time, where $\omega \in (1,2]$, TFDWE is produced from the second-order partial differential equation [2]. One of the methods used to find the solution to the time fractional differential equation is the B-spline method, due to the ease of use and accuracy of the results [11,16,5,34], which leads to ease of finding the solution through the computer [2]. Schoenberg initially presented the trigonometric spline function in 1964 [20]. A non polynomial B-spline function with trigonometric terms is called a trigonometric B-spline. Trigonometric B-spline's attributes and derivation were discovered in [41]. In this study we will solve the system (1.1) using the hybrid B-spline technique (HB-spline). To solve TFDWE this study, Caputo time fractional derivative definition was used and it was approximated using finite differences, while the HB-spline method was used to approximate the solution and derivatives with respect to r. Finding analysis and approximation solutions to TFPDE is of interest to a number of researchers, especially in recent years, and several studies have been presented, including fractional diffusion wave equation for time with damping, Chen et al. [12,16] presented the technique of variable separation by application the implicit difference of Legendre wavelets [19].
While spectral methods perform better in smooth, periodic settings, HB-splines dominate adaptive geometric modeling. Geometric constraints, adaptivity requirements, and problem smoothness all influence the decision. In the future, hybrid approaches might close this gap. The following points summarize the numerical challenges we may encounter in our study and provide strategies for overcoming them [17]:

- Traditional methods of numerical integration may lose accuracy when approaching the singularity, so specialized methods are used that stepwise divide the time and transform the singularity into an analytically integrable form.
- The method used in the research, we did not need fast convolution methods or sum of exponents techniques because our analysis method converts the Caputo integral to a sum.
- Calculating stability using classical methods is difficult for fractional equations, but calculating stability was unconditional in our work.

- To remove the singular solution when $t = 0$, we increased the point density and automatically adjusted the step size Δt based on the solution behavior.

The manuscript is divided as follows: The section 2 provides a brief overview of the method HB-spline, while the section 3 explains the numerical approach for the proposed method. The stability of the method is studied in the section 4. Numerical applications are discussed in the section 5. In the section 6, we conclude the manuscript with remarks on the results and future work.

2. The formulation of the HB-spline approaches

The fractional diffusion wave equation is solved in this study using the HB-spline. Assume that over the endowed interval $[c, d]$, the partition $\Delta : c = r_0 < r_1 < r_2 < ... < r_n - 1 < r_n = b$ such that $h = \frac{d-c}{n}$ and $r_i = c + ih$ where $i = 0(1)n$ and n is mesh size of Δ. We can now define the HB-spline using the B-spline and trigonometric B-spline approaches in the following format [6]

$$\mathbb{H}_i(r) = \theta \mathbb{B}_i(r) + (1 - \theta)\mathbb{T}_i(r), \tag{2.1}$$

where $\theta \in \mathbb{R}$, $\mathbb{B}_i(r)$ is the quartic b-spline function and $\mathbb{T}_i(r)$ is the trigonometric spline function. For further clarification, see the appendix.

First, we write the approximate solution in the following form

$$\hat{v}(r, s) = \sum_{i=-4}^{n-1} c_i \mathbb{H}_i(r), \tag{2.2}$$

where $\mathbb{H}_i(r)$ is HB-spline functions.

The formula $\hat{v}_i^j = \hat{v}(r_i, s_j)$ represents a numerical solution, where $j = 0(1)n$. The following formulas can now be used to express $\hat{v}_i^j, (\hat{v}_r)_i^j$ and $(\hat{v}_{rr})_i^j$.

$$\begin{cases} \hat{v}_i^j = l_1 c_{i-4}^j + l_2 c_{i-3}^j + l_2 c_{i-2}^j + l_1 c_{i-1}^j \\ (\hat{v}_r)_i^j = -l_3 c_{i-4}^j - l_4 c_{i-3}^j + l_4 c_{i-2}^j + l_3 c_{i-1}^j, \\ (\hat{v}_{rr})_i^j = l_5 c_{i-4}^j - l_5 c_{i-3}^j - l_5 c_{i-2}^j + l_5 c_{i-1}^{j-1}. \end{cases} \tag{2.3}$$

The time fractional diffusion wave equation is solved using the values of HB-spline functions and their derivative at the different knots, which are given in Table 1.

Table 1: The values at r_i of $\mathbb{B}_i(r)$ and their derivative

	r_{i-2}	r_{i-1}	r_i	r_{i+1}	r_{i+2}	r_{i+3}
$\mathbb{H}_i$	0	l_1	l_2	l_2	l_1	0
$\mathbb{H}_i'$	0	$-l_3$	$-l_4$	l_4	l_3	0
$\mathbb{H}_i''$	0	l_5	$-l_5$	$-l_5$	l_5	0

In Table (1), we set

$$
\begin{aligned}
l_1 &= \frac{\theta}{24} + \frac{(1-\theta)}{\vartheta} z_1, \\
l_2 &= \frac{11\theta}{24} + \frac{(1-\theta)}{\vartheta} z_2, \\
l_3 &= \frac{\theta}{6h} + \frac{(1-\theta)}{\vartheta} z_3, \\
l_4 &= \frac{\theta}{2h} + \frac{(1-\theta)}{\vartheta} z_4, \\
l_5 &= \frac{\theta}{2h^2} + \frac{(1-\theta)}{\vartheta} z_5, \\
z_1 &= (\sin(\frac{h}{2}))^3 \csc(h) \csc(\frac{3h}{2}), \\
z_2 &= (\sin(\frac{h}{2}))^2 \csc(h) \csc(2h) + 2\sin(\frac{h}{2}) \sin(h) \csc(\frac{3h}{2}) \csc(2h), \\
z_3 &= \frac{\csc(h)\sec(h)}{2 + 4\cos(h)}, \\
z_4 &= \csc(2h), \\
z_5 &= \csc(h)\csc(2h).
\end{aligned}
\tag{2.4}
$$

3. Numerical Approach for TFPDE

As we mentioned earlier, the fractional derivative will be approximated using Caputo's formulation using finite differences. The following is one way to write the expression $\frac{\partial^\omega v(r,s)}{\partial s^\omega}$: Actually, we will use the central discretizations that are frequently employed to approximate partial derivatives of the second order to approximate the fractional derivative of ω order [23].

$$
\frac{\partial^\omega \hat{v}(r, s_{j+1})}{\partial s^\omega} = \frac{1}{\Gamma(3-\omega)} \sum_{\mu=0}^{j} b_\mu [\frac{\hat{v}(r, s_{j+1-\mu}) - 2\hat{v}(r, s_{j-\mu}) + \hat{v}(r, s_{j-1-\mu})}{\Delta s^\omega}] + e_{\Delta s}^{j+1}, \tag{3.1}
$$

where $s_j = j\Delta s$, $j = 0(1)m$, $\Delta s = \frac{S}{M}$, $b_\mu = (\mu+1)^{2-\omega} - \mu^{2-\omega}$ and $e_{\Delta s}^{j+1}$ is the local truncation error such that

$$
e_{\Delta s}^{j+1} \leq \sigma(\Delta s^2).
$$

The numerical accuracy of the formula (3.1) is $O((\Delta s)^{4-\omega})$. Here are some of the popular features of b_μ:

- $b_\mu > 0 \ \ and \ \ b_1 = 1, \ \ \mu = 1, 2, ..., j,$
- $b_0 \gtrsim b_1 \gtrsim ..... \gtrsim b_\mu, b_\iota \to 0 \ \ as \ \ \mu \to \infty,$
- $-b_\mu + (2b_\mu - b_{\mu-1}) + \sum_{\mu=0}^{j-1}(-b_{\mu-1} + 2b_\mu + b_{\mu+1}) + (2b_0 + b_1) = 1$

Now, substituting (3.1) in (1.1) we obtain,

$$
\begin{aligned}
&\frac{1}{\Gamma(3-\omega)} \sum_{\mu=0}^{j} b_\mu [\frac{\hat{v}(r, s_{j+1-\mu}) - 2\hat{v}(r, s_{j-\mu}) + \hat{v}(r, s_{j-1-\mu})}{\Delta s^\omega}] + \eta [\frac{\hat{v}(r, s_{j+1}) - \hat{v}(r, s_j)}{\Delta s}] \\
&+ \lambda v(r, s_{j+1}) - \frac{\partial^2 \hat{v}(r, s_{j+1})}{\partial r^2} = G(\hat{v}(r, s_{j+1})) + \phi(r, s_{j+1}).
\end{aligned}
\tag{3.2}
$$

Let $\hat{v}^{j+1} = \hat{v}(r, s_{j+1})$, $\alpha = \frac{1}{\Gamma(3-\omega)\Delta s^\omega}$ and $\beta = \frac{\eta}{\Delta s}$. The last equation can be expressed in this way:

$$
\begin{aligned}
&(\alpha + \beta + \lambda)\hat{v}^{j+1} - (2\alpha + \beta)\hat{v}^j + \alpha \hat{v}^{j-1} + \alpha \sum_{\mu=0}^{j} b_\mu [\hat{v}(r, s_{j+1-\mu}) - 2\hat{v}(r, s_{j-\mu}) + \hat{v}(r, s_{j-1-\mu})] \\
&- \frac{\partial^2 \hat{v}^{j+1}}{\partial r^2} = G(\hat{v}^{j+1}) + \phi(r, s_{j+1}), \quad j = 0(1)m,
\end{aligned}
\tag{3.3}
$$

when $j=0$ or $\mu=j$, $\hat{v}^{-1}$ emerges; Using the initial condition we can get rid of it.

$$\begin{cases} \hat{v}_t^0 = \frac{\hat{v}^1-\hat{v}^{-1}}{2\Delta s} \\ \Rightarrow \hat{v}^{-1} = \hat{v}^1 - 2\Delta s\zeta_1(r). \end{cases} \tag{3.4}$$

The equation (3.3) can be rewritten in another form by substitution (2.3) in it.

$$\begin{aligned} &[l_1(\alpha+\beta+\lambda)-l_5]c_{i-4}^{j+1}+[l_2(\alpha+\beta+\lambda)+l_5]c_{i-3}^{j+1}+[l_2(\alpha+\beta+\lambda)+l_5]c_{i-2}^{j+1}+[l_1(\alpha+\beta+\lambda)\\ &-l_5]c_{i-1}^{j+1}=(2\alpha+\beta)[l_1c_{i-4}^{j}+l_2c_{i-3}^{j}+l_2c_{i-2}^{j}+l_1c_{i-1}^{j}]-\alpha[l_1c_{i-4}^{j-1}+l_2c_{i-3}^{j-1}+l_2c_{i-2}^{j-1}+l_1c_{i-1}^{j-1}]\\ &-\alpha\sum_{\iota=1}^{j}b_\iota([l_1c_{i-4}^{j+1-\iota}+l_2c_{i-3}^{j+1-\iota}+l_2c_{i-2}^{j+1-\iota}+l_1c_{i-1}^{j+1-\iota}]-2[l_1c_{i-4}^{j-\iota}+l_2c_{i-3}^{j-\iota}+l_2c_{i-2}^{j-\iota}+l_1c_{i-1}^{j-\iota}]\\ &+[l_1c_{i-4}^{j-1-\iota}+l_2c_{i-3}^{j-1-\iota}+l_2c_{i-2}^{j-1-\iota}+l_1c_{i-1}^{j-1-\iota}])+\phi(r_i,s_{j+1})+G(l_1c_{i-4}^{j+1}+l_2c_{i-3}^{j+1}+l_2c_{i-2}^{j+1}+l_1c_{i-1}^{j+1}). \end{aligned} \tag{3.5}$$

There are $(n+1)$ equations in the system (3.5) and $(n+4)$ unknowns. As a result, we must use the boundary conditions to add two equations (1.1).

$$\begin{cases} l_1c_{-4}^{j}+l_2c_{-3}^{j}+l_2c_{-2}^{j}+l_1c_{-1}^{j}=\varsigma_0(s_{j+1}) \\ \\ l_1c_{N-4}^{j}+l_2c_{N-3}^{j}+l_2c_{N-2}^{j}+l_1c_{N-1}^{j}=\varsigma_1(s_{j+1}). \end{cases} \tag{3.6}$$

The pseudoinverse method will be used to solve the system because the number of unknowns is greater than the number of equations, which results in a non-square matrix [18].
The initial condition (1.1) will be used to determine the values of c_i^j when $j=0$ before solving the system (3.5).

$$\begin{cases} (\hat{v}_0^j)_r = \zeta_0'(r_i), i=0, \\ \\ \hat{v}_i^0 = v(r_i,0)=\zeta_0(r_i), i=0(1)n, \\ \\ (\hat{v}_i^0)_n = \zeta_0'(r_i), i=n. \end{cases} \tag{3.7}$$

Therefore, we will obtain a system consisting of $(n+3)$ of equations and $(n+4)$ of unknowns, and it can be expressed in the following formula:

$$\Upsilon C_0 = \chi, \tag{3.8}$$

where Υ, C_0, and χ are follows:

$$\Upsilon = \begin{bmatrix} -l_3 & -l_4 & l_4 & l_3 & \dots & 0 & 0 & 0 & 0 \\ l_1 & l_2 & l_2 & l_1 & \dots & 0 & 0 & 0 & 0 \\ 0 & l_1 & l_2 & l_2 & l_1 & \dots & 0 & 0 & 0 \\ \vdots & \vdots & \vdots & \vdots & \vdots & \vdots & \vdots & \vdots & \vdots \\ 0 & \dots & \dots & 0 & 0 & l_1 & l_2 & l_2 & l_1 \\ 0 & \dots & \dots & 0 & 0 & -l_3 & l-4 & l_4 & l_3 \end{bmatrix},$$

$$\chi^T = \begin{bmatrix} \frac{d}{dr}\zeta_0(r_0) & \zeta_0(r_0) & \zeta_0(r_1) & \dots & \zeta_0(r_n) & \frac{d}{dr}\zeta_0(r_n) \end{bmatrix}^T,$$

$$C_0^T = \begin{bmatrix} c_{-4}^0 & c_{-3}^0 & c_0^{-2} & \dots & c_{n-2}^0 & c_{n-1}^0 \end{bmatrix}^T.$$

4. Stability

In order to address the stability of an inhomogeneous problem, one need only demonstrate the problem's homogeneity in accordance with Duhamel's principle [39], and hence $\phi(r,s)=0$. When the mistakes disappear as the computational process proceeds, the numerical technique is stable [23]. The Fourier method will be employed to accomplish this, thus define the error term ρ_k^j as

$$\rho_k^j = b_k^j - \tilde{b}_k^j, \quad k=0(1)n, \quad j=0(1)m. \tag{4.1}$$

Where, $\tilde{b}_k^j$ is the approximation of the fourier mode and b_k^j is the growth factor of the mode. from (4.1) and (3.5),We find the roundoff error equation as follows:

$$\begin{aligned}
&[l_1(\alpha+\beta+\lambda)-l_5]\rho_{i-4}^{j+1}+[l_2(\alpha+\beta+\lambda)+l_5]\rho_{i-3}^{j+1}+[l_2(\alpha+\beta+\lambda)+l_5]\rho_{i-2}^{j+1}+[l_1(\alpha+\beta+\lambda)\\
&-l_5]\rho_{i-1}^{j+1}=(2\alpha+\beta)[l_1\rho_{i-4}^{j}+l_2\rho_{i-3}^{j}+l_2\rho_{i-2}^{j}+l_1\rho_{i-1}^{j}]-\alpha[l_1\rho_{i-4}^{j-1}+l_2\rho_{i-3}^{j-1}+l_2\rho_{i-2}^{j-1}+l_1\rho_{i-1}^{j-1}]\\
&-\alpha\sum_{\mu=1}^{j}b_\mu([l_1\rho_{i-4}^{j+1-\mu}+l_2\rho_{i-3}^{j+1-\mu}+l_2\rho_{i-2}^{j+1-\mu}+l_1\rho_{i-1}^{j+1-\mu}]-2[l_1\rho_{i-4}^{j-\mu}+l_2\rho_{i-3}^{j-\mu}+l_2\rho_{i-2}^{j-\nu}+l_1\rho_{i-1}^{j-\mu}]\\
&+[l_1\rho_{i-4}^{j-1-\mu}+l_2\rho_{i-3}^{j-1-\mu}+l_2\rho_{i-2}^{j-1-\mu}+l_1\rho_{i-1}^{j-1-\mu}])+G(l_1c_{i-4}^{j+1}+l_2c_{i-3}^{j+1}+l_2c_{i-2}^{j+1}+l_1c_{i-1}^{j+1}).
\end{aligned} \tag{4.2}$$

Now,suppose that

$$G(l_1c_{i-4}^{j+1}+l_2c_{i-3}^{j+1}+l_2c_{i-2}^{j+1}+l_1c_{i-1}^{j+1})=a(l_1c_{i-4}^{j+1}+l_2c_{i-3}^{j+1}+l_2c_{i-2}^{j+1}+l_1c_{i-1}^{j+1}).$$

In this case, a is constant. Consequently, the roundoff error equation becomes like this:

$$\begin{aligned}
&[l_1(\alpha+\beta+\lambda-a)-l_5]\rho_{i-4}^{j+1}+[l_2(\alpha+\beta+\lambda-a)+l_5]\rho_{i-3}^{j+1}+[l_2(\alpha+\beta+\lambda-a)+l_5]\rho_{i-2}^{j+1}\\
&+[l_1(\alpha+\beta+\lambda-a)-l_5]\rho_{i-1}^{j+1}=(2\alpha+\beta)[l_1\rho_{i-4}^{j}+l_2\rho_{i-3}^{j}+l_2\rho_{i-2}^{j}+l_1\rho_{i-1}^{j}]-\alpha[l_1\rho_{i-4}^{j-1}\\
&+l_2\rho_{i-3}^{j-1}+l_2\rho_{i-2}^{j-1}+l_1\rho_{i-1}^{j-1}]-\alpha\sum_{\mu=1}^{j}b_\mu([l_1\rho_{i-4}^{j+1-\mu}+l_2\rho_{i-3}^{j+1-\mu}+l_2\rho_{i-2}^{j+1-\mu}+l_1\rho_{i-1}^{j+1-\mu}]\\
&-2[l_1\rho_{i-4}^{j-\mu}+l_2\rho_{i-3}^{j-\mu}+l_2\rho_{i-2}^{j-\nu}+l_1\rho_{i-1}^{j-\mu}]+[l_1\rho_{i-4}^{j-1-\mu}+l_2\rho_{i-3}^{j-1-\mu}+l_2\rho_{i-2}^{j-1-\mu}+l_1\rho_{i-1}^{j-1-\mu}]).
\end{aligned} \tag{4.3}$$

The boundary conditions of the equation (4.3) are

$$\rho_0^j=g_0(s_j), \quad \rho_n^j=g_1(s_j), \quad j=0(1)m. \tag{4.4}$$

And the initial conditions

$$\rho_k^0=h_0(r_k), \quad (\rho_s)_k^0=h_1(r_k), \quad k=0(1)n. \tag{4.5}$$

Define the grid function [42]

$$\rho^j(r)=\begin{cases}\rho_k^j, & r_k-\frac{h}{2}<r\le r_k+\frac{h}{2}, \quad k=0(1)n,\\ 0, & c<r<\frac{h}{2} \ \ or \ \ d-\frac{h}{2}<r<d.\end{cases} \tag{4.6}$$

$\rho^j(r)$'s Fourier series can be formed as

$$\rho^j(r)=\sum_{\nu=-\infty}^{\infty}\zeta^j(\nu)e^{\frac{i2\pi\nu r}{(d-c)}}, \quad j=0(1)n. \tag{4.7}$$

where,

$$\zeta^j(\nu)=\frac{1}{(d-c)}\int_c^d\rho^j(r)e^{\frac{-i2\pi\nu r}{(d-c)}}dr. \tag{4.8}$$

Let $\rho^j = [\rho_1^j, \rho_2^j, ..., \rho_{n-1}^j]^T$,

and introduce the norm [21]

$$\|\rho^j\|_2 = (\sum_{j=1}^{m-1} h|\rho_k^j|^2)^{\frac{1}{2}} = [\int_c^d |\rho_k^j|^2 dr]^{\frac{1}{2}}. \tag{4.9}$$

Parseval's equality makes it evident that $\int_c^d |\rho_k^j|^2 dx = \sum_{\nu=-\infty}^{\infty} |\zeta^j(\nu)|^2$

Consequently, the following relationship is obtained:

$$\|\rho^j\|_2^2 = \sum_{\nu=-\infty}^{\infty} |\zeta^j(\nu)|^2. \tag{4.10}$$

Now,we assume that $\rho_k^j = \zeta^j e^{ipkh}$ is solution of the equations (4.3) -(4.5),where $i = \sqrt{-1}$ and p is real. Thus, the following is one way to write the equation (4.3).

$$\begin{aligned}
&[l_1(\alpha+\beta+\lambda-a)-l_5]\zeta^{j+1}e^{ip(k-4)h} + [l_2(\alpha+\beta+\lambda-a)+l_5]\zeta^{j+1}e^{ip(k-3)h} + [l_2(\alpha+\beta+\lambda-a)+l_5]\zeta^{j+1}e^{ip(k-2)h} \\
&+ [l_1(\alpha+\beta+\lambda-a)-l_5]\zeta^{j+1}e^{ip(k-1)h} = (2\alpha+\beta)[l_1\zeta^j e^{ip(k-4)h} + l_2\zeta^j e^{ip(k-3)h} + l_2\zeta^j e^{ip(k-2)h} + l_1\zeta^j e^{ip(k-1)h}] \\
&- \alpha[l_1\zeta^{j-1}e^{ip(k-4)h} + l_2\zeta^{j-1}e^{ip(k-3)h} + l_2\zeta^{j-1}e^{ip(k-2)h} + l_1\zeta^{j-1}e^{ip(k-1)h}] \\
&- \alpha[l_1 e^{ip(k-4)h} + l_2 e^{ip(k-3)h} + l_2 e^{ip(k-2)h} + l_1 e^{ip(k-1)h}] \sum_{\mu=1}^{j} b_\mu(\zeta^{j+1-\mu} - 2\zeta^{j-\mu} + \zeta^{j-1-\mu}).
\end{aligned} \tag{4.11}$$

We divide (4.11)on e^{ipkh} ,so it becomes as follows

$$\zeta^{j+1} = 2\tau\zeta^j - \omega\zeta^{j-1} - \omega\sum_{\mu=1}^{j} b_\mu(\zeta^{j+1-\mu} - 2\zeta^{j-\mu} + \zeta^{j-1-\mu}). \tag{4.12}$$

Where, $\gamma = \frac{[l_1 e^{-3iph} + l_2 e^{-2iph} + l_2 e^{-iph} + l_1]}{(\alpha+\frac{\beta}{2})^{-1}[r_1 e^{-3iph} + r_2 e^{-2iph} + r_2 e^{-iph} + r_1]}$, and $\psi = \frac{[l_1 e^{-3iph} + l_2 e^{-2iph} + l_2 e^{-iph} + l_1]}{(\alpha)^{-1}[r_1 e^{-3iph} + r_2 e^{-2iph} + r_2 e^{-iph} + r_1]}$,
where $r_1 = [l_1(\alpha+\beta+\lambda-a) - l_5]$, and $r_2 = [l_2(\alpha+\beta+\lambda-a) + l_5]$.

Clearly $\gamma \leq 1$ at $(\alpha+\frac{\beta}{2})^{-1}r_1 \geq l_1$ and $(\alpha+\frac{\beta}{2})^{-1}r_2 \geq l_2$, and also $\psi \leq 1$ at $(\alpha)^{-1}r_1 \geq l_1$ and $(\alpha)^{-1}r_2 \geq l_2$.

Lemma 4.1 *If there is a ζ^j solution to the equation (4.12), then $|\zeta^j| \leq 2|\zeta^0|$, $j = 0(1)m$.*
proof: We now demonstrate the result by induction, For $j = 0$, the equation (4.12) implies $\zeta^j = 2\gamma\zeta^0$ since $\gamma \leq 1$ then, $|\zeta^j| \leq 2|\zeta^0|$.
Now, $|\zeta^j| \leq 2|\zeta^0|$, $j = 0, 1, 2, ...m-1$.so that from (4.12) we obtain

$$|\zeta^{j+1}| = 2\gamma|\zeta^j| - \psi|\zeta^{j-1}| - \psi\sum_{r=1}^{j} b_r(|\zeta^{j+1-r}| - 2|\zeta^{j-r}| + |\zeta^{j-1-r}|)$$

$$\rightarrow |\zeta^{j+1}| \leq 2\tau|\zeta^0| - 2\psi|\zeta^0| - 2\psi\sum_{r=1}^{j} b_r(|\zeta^0| - 2|\zeta^0| + |\zeta^0|)$$

$$\rightarrow |\zeta^{j+1}| \leq 2|\zeta^0|$$

Theorem 4.1 *(3.5) has unconditional system stability.*
proof: From Lemma (4.1) and (4.10) allow us to proceed to $\|\rho^j\|_2 \leq 2\|\rho^0\|_2$, $j = 0(1)m$. This indicates that the system (3.5) is unconditionally stable.

5. Numerical Application

This section provides examples of how to solve TFDWE in order to make the solution techniques more understandable. To show the accuracy of the numerical solution we obtained, we determine the problem's

analysis solution. By comparing the numerical and analysis solutions, We can verify that the numerical results are accurate and legitimate. We utilized Maple 15 to solve the problems. The error norms L_2, and L_∞ are used to test the accuracy of the method that is being described. which are computed in [38] as follows,

$$L_2 = \|v - \hat{v}_n\|_2 \simeq \sqrt{h \sum_{j=0}^{n} |v_j - (\hat{v}_n)_j|^2},$$

and

$$L_\infty = \|v - \hat{v}_n\|_\infty \simeq max_j |v_j - (\hat{v}_n)_j|.$$

Example 1 In this example we are dealing with TFDWE ,

$$\begin{aligned} &\frac{\partial^\omega v(r,s)}{\partial s^\omega} + v(r,s) - \frac{\partial^2 v(r,s)}{\partial r^2} + v^2(r,s) = \phi(r,s), \\ &v(r,0) = 0, \quad \frac{\partial v(r,0)}{\partial s} = 0, \qquad\qquad r \in [0,1], \\ &v(0,s) = 0 \quad and \quad v(1,s) = s^2 \sin(1), \qquad s \in [0,1], \end{aligned} \tag{5.1}$$

where, $\phi(r,s) = \frac{2s^{2-\omega}\sinh(r)}{\Gamma(3-\omega)} + s^4 \sinh^2(r)$ the analysis solution of problem (5.1) is $v(r,s) = s^2 \sinh(r)$. Tables 2 and 3 display the absolute errors for different values of Δ s and $n = 30$ and $n = 60$, respectively. Figure 1 compares the approximate solution with the analytical solution for $\omega = 1.5$ and $s = 0.01$, while Figure 2 displays the approximate solution for various time values. and the approximate answer for various values of ω is displayed in Figure 3. We can conclude that our findings closely match the exact solution.

Table 2: The L^∞ and L^2 errors with different values for Δs and n=30 for Example 1.

Δs	L^∞	L^2
0.01	$6.6846 * 10^{-7}$	$1.3728 * 10^{-5}$
0.05	$1.2344 * 10^{-5}$	$3.968 * 10^{-4}$
0.09	$2.5767 * 10^{-4}$	$2.4193 * 10^{-3}$

Table 3: The L^∞ and L^2 errors with different values for Δs and n=60 for Example 1.

Δs	L^∞	L^2
0.01	$5.4902 * 10^{-7}$	$1.0145 * 10^{-5}$
0.05	$1.5148 * 10^{-5}$	$3.2468 * 10^{-4}$
0.09	$2.3827 * 10^{-4}$	$3.2858 * 10^{-3}$

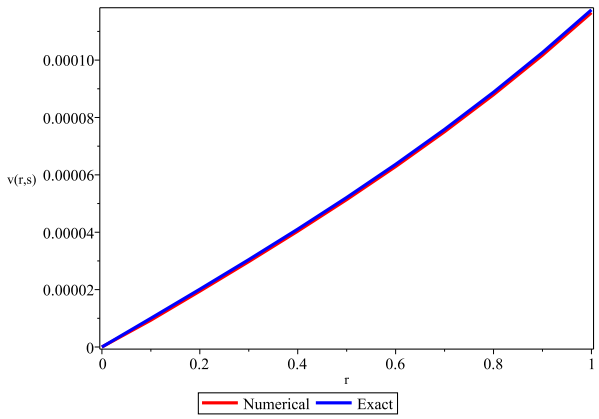

Figure 1: comparative between the exact and numerical solutions at $\omega = 1.5$ and $\theta = 0.8$.

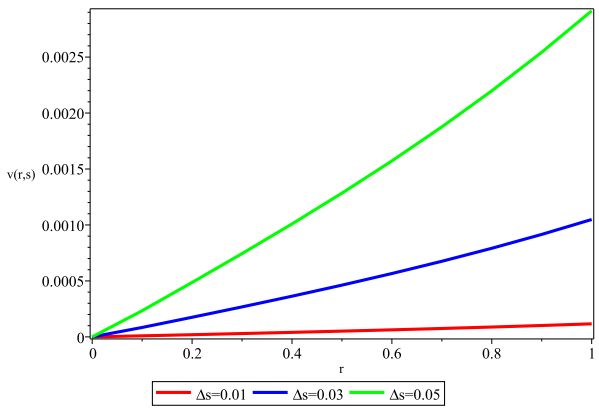

Figure 2: comparative plot at various time levels.

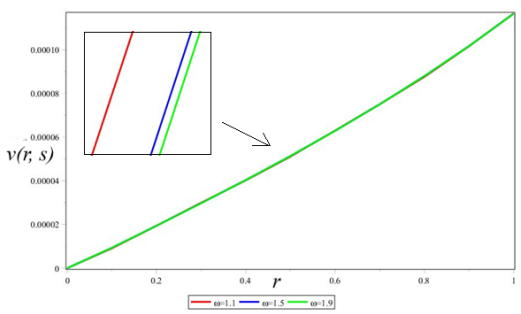

Figure 3: Numerical solutions for different values of ω for Example 1.

Example 2 We adopt the following TFDWE ,

$$\begin{aligned} &\frac{\partial^{\omega} v(r,s)}{\partial s^{\omega}} + v(r,s) - \frac{\partial^2 v(r,s)}{\partial r^2} = \phi(r,s), \\ &v(r,0) = 0, \quad \frac{\partial v(r,0)}{\partial s} = 0, \qquad\qquad r \in [0,1], \\ &v(0,s) = 0 \quad and \quad v(1,s) = 0, \qquad\qquad s \in [0,1]. \end{aligned} \tag{5.2}$$

where, $\phi(r,s) = \frac{2s^{2-\omega} r(1-r)}{\Gamma(3-\omega)} + s^2 r(1-r) + 2s^2$ The analysis solution of problem (5.2) is $v(r,s) = s^2 r(1-r)$. Figure 4 compares the approximate solution with the analytical solution for $\omega = 1.5$ and $s = 0.01$, while Figure 5 displays the approximate solution for various time values, the findings show that they are in good agreement and the approximate answer for various values of ω is displayed in Figure 6.

Table 4: The L^{∞} and L^2 errors with different values for θ and n=60 for Example 2.

θ	L^{∞}	L^2
0.5	$8.2722 * 10^{-7}$	$1.3954 * 10^{-5}$
0.9	$1.6544 * 10^{-7}$	$2.7908 * 10^{-6}$
1.5	$8.2722 * 10^{-7}$	$1.3954 * 10^{-5}$

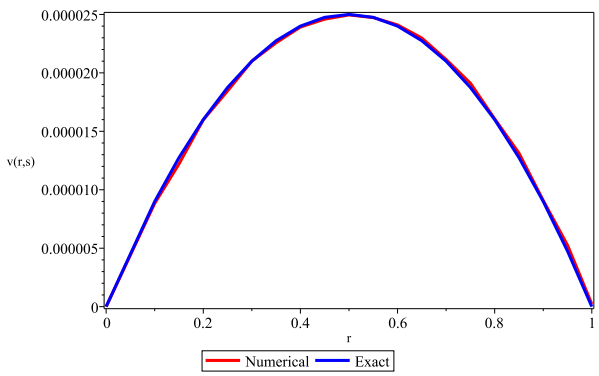

Figure 4: comparative between the exact and numerical solutions at $\omega = 1.5$ and $\theta = 0.9$.

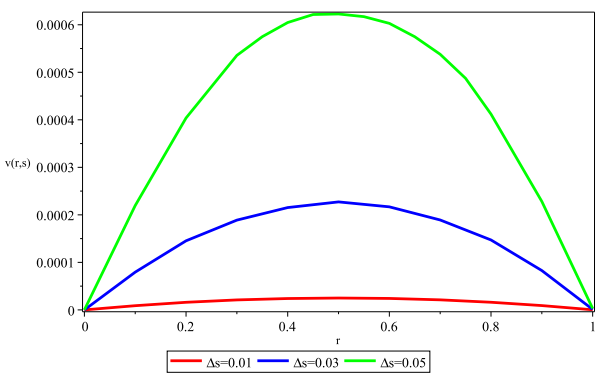

Figure 5: comparative plot at various time levels.

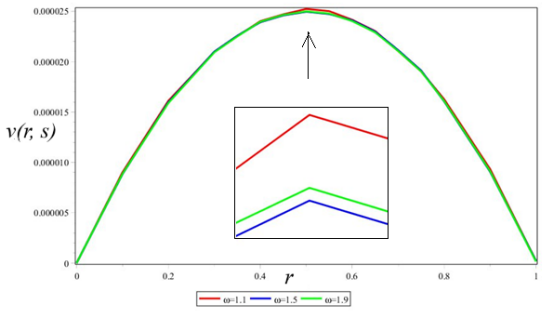

Figure 6: Numerical solutions for different values of ω for Example 2.

Acknowledgment

Thanks and appreciation to all who contributed to the completion of this study.

6. Conclusions

The spline function is a recognised and effective instrument for approximating solutions of fractional partial differential equations, due to its piecewise polynomial framework and inherent smoothness characteristics. This study presents the development and thorough analysis of an innovative HB-spline method for addressing TFDWE. Our scheme integrates the localised adaptability of quartic B-splines in the spatial dimension with a Fourier spectral approach in time, thereby converting the original fractional differential operator into a sparse, banded system of algebraic equations.

Comprehensive numerical experiments were conducted on two benchmark problems with varying fractional orders $\omega \in (0, 1)$ and distinct spatial domains. In every instance, the HB-spline method exhibited swift convergence: as the mesh was refined, the L^2 and L^∞ error norms diminished at rates commensurate with the spline's fourth-order spatial accuracy. Furthermore, the Fourier spectral discretisation in time attained spectral-level convergence for smooth data. Collectively, these findings validate that our method achieves the specified precision while operating more efficiently than conventional finite-difference or lower-order spline techniques.

A significant theoretical outcome is the demonstration of unconditional stability within the proposed HB-spline Fourier framework. In contrast to numerous time-stepping methods that necessitate adherence to the Courant-Friedrichs-Lewy condition, our algorithm maintains stability for any selection of time and spatial discretizations. This robustness is especially advantageous for addressing long-term integration issues or when utilising adaptive meshes to capture localised features.

Compared to current numerical methods such as the L1 finite-difference scheme or collocation with lower-degree splines the hybrid quartic B-spline approach demonstrates significantly lower computational expenses for a specified error tolerance. The minimal structure of the resultant linear systems facilitates efficient implementations with band-matrix solvers, while parallelisation during the Fourier transform phase enhances the speed of large-scale simulations.

Anticipating future developments, the adaptability of the HB-spline framework presents numerous promising opportunities:

- Extension to multidimensional issues and irregular geometries through tensor-product splines or spline spaces on unstructured meshes.
- Employing adaptive time-stepping strategies to improve efficiency for problems characterised by multi-scale temporal dynamics.
- Application to additional categories of fractional models, including nonlinear reaction-diffusion equations and space-fractional operators.

The proposed HB-spline method serves as a robust and efficient instrument for numerically solving a wide range of time-fractional differential equations.

References

1. Abu Arqub, O. and Maayah, B. *Retracted article: Solutions of bagley-torvik and painleve equations of fractional order using iterative reproducing kernel algorithm with error estimates.* Neural Computing and Applications 29(5) 1465–1479 (2016).

2. Abu Arqub, O., Tayebi, S., Baleanu, D., Osman, M., Mahmoud, W., and Alsulami, H. *A numerical combined algorithm in cubic b-spline method and finite difference technique for the time-fractional nonlinear diffusion wave equation with reaction and damping terms.* Results in Physics 41 105912 (2022).

3. Adomian, G. *Nonlinear Stochastic Operator Equations.* Elsevier Science, Burlington (2014). Description based upon print version of record.

4. Ahmad, B. and Ntouyas, S. *Existence of solutions for fractional differential inclusions with four-point nonlocal riemann-liouville type integral boundary conditions.* Univerzitet u Nisu. Prirodno-Matematicki Fakultet. Filomat 27(6) 1027–1036 (2013).

5. AlHumedi, H. O. *Combining b-spline least-square schemes with different weight functions to solve the generalized regularized long wave equation.* International Journal of Nonlinear Analysis and Applications 13 (2022).

6. Anuar, H. S. S., Mafazi, N. H., Hamid, N. N. A., Majid, A. A., and Azmi, A. *Solving dym equation using quartic b-spline and quartic trigonometric b-spline collocation methods.* In *AIP Conference Proceedings*, volume 1870, (040028). Author(s) (2017).

7. Arqub, O. A., Rabah, A. B., and Momani, S. *A spline construction scheme for numerically solving fractional bagley-torvik and painleve models correlating initial value problems concerning the caputo-fabrizio derivative approach.* International Journal of Modern Physics C 34(09) (2023).

8. Bahaa, G. *Fractional optimal control problem for differential system with control constraints.* Univerzitet u Nisu. Prirodno-Matematicki Fakultet. Filomat 30(8) 2177–2189 (2016).

9. Beghin, L. and Orsingher, E. *Fractional poisson processes and related planar random motions.* Electronic Journal of Probability 14(none) (2009).

10. Benson, D. A., Wheatcraft, S. W., and Meerschaert, M. M. *Application of a fractional advection-dispersion equation.* Water Resources Research 36(6) 1403–1412 (2000).

11. Bloshi, Z. S. and Taha, B. A. *Cubic b-splines method for solving singularly perturbed delay partial differential equations.* Journal of Al-Qadisiyah for Computer Science and Mathematics 13(3) (2021).

12. Chen, J., Liu, F., Anh, V., Shen, S., Liu, Q., and Liao, C. *The analytical solution and numerical solution of the fractional diffusion-wave equation with damping.* Applied Mathematics and Computation 219(4) 1737–1748 (2012).

13. Ding, Q. and Wong, P. J. Y. *Numerical method for fractional bagley-torvik equation.* In *Central European Symposium on Thermophysics 2019 (CEST)*, volume 2133, (240007). AIP Publishing (2019).

14. Ding, Q. and Wong, P. J. Y. *A higher order numerical scheme for solving fractional bagley-torvik equation.* Mathematicsl Methods in the Applied Sciences 45(3) 1241–1258 (2021).

15. Djida, J., Atangana, A., and Area, I. *Numerical computation of a fractional derivative with non-local and non-singular kernel.* Mathematical Modelling of Natural Phenomena 12(3) 4–13 (2017).

16. Farhood, A. K., Mohammed, O. H., and Taha, B. A. *Solving fractional time-delay diffusion equation with variable-order derivative based on shifted legendre-laguerre operational matrices.* Arabian Journal of Mathematics 12(3) 529–539 (2023).

17. Fei, M. and Huang, C. *Galerkin-Legendre spectral method for the distributed-order time fractional fourth-order partial differential equation.* International Journal of Computer Mathematics 97(6) 1183–1196 (2019).

18. Ford, W. *Numerical linear algebra with applications.* Academic Press, London, first edition edition (2015). Includes index.

19. Heydari, M., Hooshmandasl, M., Maalek Ghaini, F., and Cattani, C. *Wavelets method for the time fractional diffusion-wave equation.* Physics Letters A 379(3) 71–76 (2015).

20. Hussain, M. Z., Abbas, S., and Irshad, M. *Quadratic trigonometric b-spline for image interpolation using ga.* PLOS One 12(6) e0179721 (2017).

21. Johnson, L. W. and Riess, R. D. *Numerical analysis.* Addison-Wesley, Reading, Mass. [u.a.], 2. ed. edition (1982).

22. Khalaf, S. L., Kassid, K. K., and Khudair, A. R. *A numerical method for solving quadratic fractional optimal control problems.* Results in Control and Optimization 13 100330 (2023).

23. Khalid, N., Abbas, M., Iqbal, M. K., and Baleanu, D. *A numerical algorithm based on modified extended b-spline functions for solving time-fractional diffusion wave equation involving reaction and damping terms.* Advances in Difference Equations 2019(1) (2019).

24. Mahdi, N. and Khudair, A. *Some delta q-fractional linear dynamic equations and a generalized delta q-mittag-leffler function.* Computational Methods for Differential Equations (2023).

25. Mahdi, N. K. and Khudair, A. R. *An analytical method for q-fractional dynamical equations on time scales.* Partial Differential Equations in Applied Mathematics 8 100585 (2023).

26. Mahdi, N. K. and Khudair, A. R. *The delta q-fractional gronwall inequality on time scale.* Results in Control and Optimization 12 100247 (2023).

27. Mahdi, N. K. and Khudair, A. R. *Linear fractional dynamic equations: Hyers-ulam stability analysis on time scale.* Results in Control and Optimization 14 100347 (2024).

28. Mahdi, N. K. and Khudair, A. R. *Toward stability investigation of fractional dynamical systems on time scale.* Turkish World Mathematical Society Journal of Applied and Engineering Mathematics 14(4) 1495–1513 (2024).

29. Mahdi, N. K. and Khudair, A. R. *Some analytical results on the Δ-fractional dynamic equations.* Turkish World Mathematical Society Journal of Applied and Engineering Mathematics 15 577–589 (2025).

30. Meerschaert, M. M. and Scalas, E. *Coupled continuous time random walks in finance* (2006).

31. Meerschaert, M. M. and Tadjeran, C. *Finite difference approximations for fractional advection dispersion flow equations.* Journal of Computational and Applied Mathematics 172(1) 65–77 (2004).

32. Miller, K. S. and Ross, B. *An introduction to the fractional calculus and fractional differential equations.* A @Wiley-Interscience publication. Wiley, New York [u.a.] (1993). Literaturverz. S. 357 - 360.

33. Mohammed, J. K. and Khudair, A. *Numerical solution of fractional integro-differential equations via fourth-degree hat functions.* Iraqi Journal for Computer Science and Mathematics (10–30) (2023).

34. Nashmi, F. K. and Taha, B. A. *Numerical study of the time-fractional partial differential equations by using quartic b-spline method.* Partial Differential Equations in Applied Mathematics 12 101008 (2024).

35. Podlubny, I. *Fractional differential equations.* Number v. 198 in Mathematics in science and engineering. Academic Press, San Diego (1999). Includes bibliographical references (p. 313-335) and index.

36. Roul, P. and Goura, V. P. *A high-order b-spline collocation scheme for solving a nonhomogeneous time-fractional diffusion equation.* Mathematicsl Methods in the Applied Sciences 44(1) 546–567 (2020).

37. Sakar, M. G., Saldir, O., and Akgul, A. *A novel technique for fractional bagley-torvik equation.* Proceedings of the National Academy of Sciences, India Section A: Physical Sciences 89(3) 539–545 (2018).

38. Siddiqi, A. H. *Functional Analysis and Applications.* Springer Singapore (2018).

39. Strikwerda, J. C. *Finite difference schemes and partial differential equations.* Number 88 in Other titles in applied mathematics. Society for Industrial and Applied Mathematics (SIAM, 3600 Market Street, Floor 6, Philadelphia, PA 19104), Philadelphia, Pa, 2nd ed edition (2004). Restricted to subscribers or individual electronic text purchasers.

40. Tamsir, M., Dhiman, N., Nigam, D., and Chauhan, A. *Approximation of caputo time-fractional diffusion equation using redefined cubic exponential b-spline collocation technique.* AIMS Mathematics 6(4) 3805–3820 (2021).

41. Walz, G. *Identities for trigonometric b-splines with an application to curve design.* BIT Numerical Mathematics 37(1) 189–201 (1997).

42. Yaseen, M., Abbas, M., Nazir, T., and Baleanu, D. *A finite difference scheme based on cubic trigonometric b-splines for a time fractional diffusion-wave equation.* Advances in Difference Equations 2017(1) (2017).

43. Zhang, W., Cai, X., and Holm, S. *Time-fractional heat equations and negative absolute temperatures.* Computers & Mathematics with Applications 67(1) 164–171 (2014).

Appendix

Define the HB-spline using the B-spline and trigonometric B-spline approaches in the following format [6]

$$\mathbb{H}_i(r) = \begin{cases} \mathrm{J}_1, & \text{if } r \in [r_{i-2}, r_{i-1}], \\ \mathrm{J}_2, & \text{if } r \in [r_{i-1}, r_i], \\ \mathrm{J}_3, & \text{if } r \in [r_i, r_{i+1}], \\ \mathrm{J}_4, & \text{if } r \in [r_{i+1}, r_{i+2}], \\ \mathrm{J}_5, & \text{if } r \in [r_{i+2}, r_{i+3}], \\ 0, & \text{otherwise.} \end{cases}$$

where,

$$\mathrm{J}_1 = \frac{\theta}{24h^4}(r - r_{i-2})^4 + \frac{(1-\theta)}{\vartheta} f^4(r_i),$$

$$\mathrm{J}_2 = \frac{\theta}{24h^4}[h^4 + 4h^3(r - r_{i-1}) + 6h^2(r - r_{i-1})^2 + 4h(r - r_{i-1})^3 - 4(r - r_{i-1})^4] + \frac{(1-\theta)}{\vartheta}[f^3(r_i)g(r_{i+2}) + f^2(r_i)g(r_{i+3})f(r_{i+1}) + f(r_i)g(r_{i+4})f^2(r_{i+1}) + g(r_{i+5})f^3(r_{i+1})],$$

$$\mathrm{J}_3 = \frac{\theta}{24h^4}[11h^4 + 12h^3(r - r_{i-1}) - 6h^2(r - r_{i-1})^2 + 12h(r - r_{i-1})^3 + 6(r - r_{i-1})^4] + \frac{(1-\theta)}{\vartheta}[f^2(r_i) g^2(r_{i+3}) + f(r_i)g(r_{i+4})f(r_{i+1})g(r_{i+3}) + f(r_i)g^2(r_{i+4})f(r_{i+2}) + g(r_{i+5})f^2(r_{i+1})g(r_{i+3}) + g(r_{i+5})f(r_{i+1}) g(r_{i+4})f(r_{i+2}) + g^2(r_{i+5})f^2(r_{i+2})],$$

$$\mathrm{J}_4 = \frac{\theta}{24h^4}[h^4 + 4h^3(r_{i+2} - r) + 6h^2(r_{i+2} - r)^2 + 4h(r_{i+2} - r)^3 - 4(r_{i+2} - r)^4] + \frac{(1-\theta)}{\vartheta}[f(r_i)g^3(r_{i+3}) + g(r_{i+5})f(r_{i+1})g^2(r_{i+4}) + g^2(r_{i+5})f(r_{i+2})g(r_{i+4}) + g^3(r_{i+5})f(r_{i+3})],$$

$$\mathrm{J}_5 = \frac{\theta}{24h^4}(r_{i+3} - r)^4 + \frac{(1-\theta)}{\vartheta} g^4(r_{i+5}).$$

and, $f(r_i) = \sin(\frac{r-r_i}{2})$, $g(r_i) = \sin(\frac{r_i-r}{2})$, $\vartheta = \sin(\frac{h}{2})\sin(h)\sin(\frac{3h}{2})\sin(2h)$, $\theta > 0$.

Fahad K. Nashmi and Bushra A.Taha,
Department of Mathematics,
College of Sciences,
University of Basrah, Basrah, Iraq.
E-mail address: fahad.nashmi@uobasrah.edu.iq